

## Dalton Transactions

# Synthesis and anion binding properties of (thio)urea functionalized Ni(II)-salen complexes

Journal:	Dalton Transactions
Manuscript ID	DT-ART-09-2024-002683.R1
Article Type:	Paper
Date Submitted by the Author:	22-Oct-2024
Complete List of Authors:	Payong, Jae Elise L.; University of California Irvine Leonard, Nadia; University of California Santa Barbara, Chemistry and Biochemistry Anderson-Sanchez, Lauren; University of California Irvine Ziller, Joseph; University of California Irvine, Department of Chemistry Yang, Jenny; University of California Irvine, Chemistry

SCHOLARONE™ Manuscripts

### **ARTICLE**

# Synthesis and anion binding properties of (thio)urea functionalized Ni(II)-salen complexes

Received 00th January 20xx, Accepted 00th January 20xx

DOI: 10.1039/x0xx000000x

Jae Elise L. Payong <sup>a</sup>, Nadia G. Léonard <sup>b</sup>, Lauren M. Anderson-Sanchez <sup>a</sup>, Joseph W. Ziller <sup>a</sup>, and Jenny Y.Yang <sup>a†</sup>

Salen ligands (salen = N,N'-ethylenebis(salicylimine)) are well-known for their versatility and widespread utility in chelating metal complexes. However, installation of hydrogen-bonding units on the salen framework, particularly functional groups that require amine-based precursors such as (thio)ureas, are difficult to achieve without the use of protecting group strategies. In this report, we show that the phenylketone analog of salicyladehyde is a stable alternative that enables the facile installation of hydrogen bonding (thio)urea groups on the salen scaffold, thus imparting anion binding abilities to a metal salen complex. Synthesis of symmetric N-phenyl(thio)urea salen ligands functionalized at the 3,3'-position and an unsymmetric salen ligand with N-phenylurea at the 5-position were achieved. Subsequent metalation with nickel(II) acetate afforded the nickel(II) complexes that were investigated for their anion binding properties towards  $F^-$ ,  $CI^-$ ,  $BF^-$ ,  $CH_3COO^-$ , and  $H_2PO_4^-$ . Solid-state structures of the nickel(II) complexes as well as the  $CI^-$  bound dimer of the symmetric urea complex were obtained. The unusual acidity of the (thio)urea groups is reflected in the  $pK_8$ -dependent anion binding behavior of the nickel(II) complexes, as elucidated by  $^1H$  and  $^{19}F$  Nuclear Magnetic Resonance (NMR) spectroscopy and Diffusion Ordered Spectroscopy (DOSY) experiments.

#### Introduction

The binding, transport, and release of anions play an important role in the homeostasis of biological systems, <sup>1,2</sup> enhancing the efficiency of numerous chemical syntheses, <sup>3,4</sup> and the sensing and remediation of ionic contaminants. <sup>5–7</sup> Synthetic anion binding systems have been developed over the past few decades to understand these processes. <sup>8–12</sup>

Salen-type ligands (salen = *N,N'*-ethylenebis(salicylimine)) have been extensively studied because of their ability to coordinate to a wide range of transition metals, and they are easily synthesized through the condensation of a diamine and a salicylaldehyde or a salicylaldehyde derivative. <sup>13,14</sup> However, this synthetic pathway also leads to challenges in installing common hydrogen bonding anion binding motifs, particularly units that are built upon N–H fragments. Prior studies that describe the installation of amine groups on the salen ligand or its precursor salicylaldehyde have required the use of protecting groups to mask the amine from unwanted reactivity towards the aldehyde or to prevent the acidic phenol from interfering with the reaction. <sup>15–17</sup> These additional steps lower

the overall yield and limit the practicality of using metal salen complexes for anion binding.

Reports of metal salen complexes specifically designed for anion binding are scarce. Reinhoudt and coworkers developed a library of uranyl salen and salophen complexes, with the highly Lewis acidic  $\mathsf{U^{VI}O_2}$  center as the main site for anion binding.  $^{16-19}$  Ligands that were functionalized with pendant amide groups in the 3,3'-position demonstrated enhanced binding affinity to the anions. Tasker and coworkers approached the synthetic challenge by installing *N*-morpholinomethyl and *N*-piperidinomethyl groups at the 3,3'-position.  $^{20,21}$  The ligand was active towards the binding of  $\mathsf{SO_4^{2-}}$  at low pH when the amine is protonated to ammonium, and deprotonation of the ammonium at high pH reversed the binding of  $\mathsf{SO_4^{2-}}$ .

Beyond anion sensing and sequestration, there is also interest in installing anion binding units on metal salen complexes for synthetic applications. Nozaki and coworkers demonstrated that a *N*-piperidinomethyl functionalized cobalt(III) salen has the ability to disfavor the production of unwanted cyclic propylene carbonates in the copolymerization of CO<sub>2</sub> and various epoxides by utilizing the protonated piperidinium to suppress the nucleophilicity of the terminal carbonate from proceeding with the undesired intramolecular cyclization.<sup>22</sup> Lee and coworkers expanded on the strategy of using anion-binding motifs to disfavor the backbiting in the CO<sub>2</sub>/epoxide copolymerization by installing alkylammonium arms in the 5,5'-position of the cobalt(III) salen catalyst.<sup>23</sup>

Herein, we report the synthesis of salen ligands containing (thio)urea functional groups and their anion binding properties

Crystallographic structures (CIF) and Electronic Supplementary Information (ESI) available: experimental methods, synthetic procedures, crystallographic information, anion-specific titration curves, relevant NMR spectra, and Job plots. See DOI: 10.1039/x0xx00000x

<sup>&</sup>lt;sup>a.</sup> Department of Chemistry, University of California, Irvine, Irvine, California 92697, United States.

b. Department of Chemistry and Biochemistry, University of California, Santa Barbara, Santa Barbara, California 93106, United States.

<sup>†</sup> Corresponding Author.

ARTICLE Journal Name

Scheme 1. Synthetic pathway to access the symmetric urea and thiourea functionalized salen ligands, and their subsequent metalation with nickel(II)

Scheme 2. Synthetic pathway to access the unsymmetric urea salen ligand and its subsequent metalation with nickel(II).

as nickel(II) complexes. Nickel(II) was selected for metalation because of its diamagnetic properties, the stability of the complexes under aerobic conditions, and its inertness towards the coordination of anions in the primary sphere. Key to our synthetic approach in the installation of anion binding units is the use of the more stable precursor, 1-(3-amino-2hydroxyphenyl)ethenone. Although the ketone functional group reacts similar to its aldehyde analog in the condensation reaction, its use in the synthesis of salen-type ligands has been limited. <sup>24–27</sup> The binding properties of the nickel(II) complexes to the tetrabutylammonium (TBA) salts of F-, Cl-, Br-, CH<sub>3</sub>COO-, and H<sub>2</sub>PO<sub>4</sub><sup>-</sup> were investigated using <sup>1</sup>H and <sup>19</sup>F Nuclear Magnetic Resonance (NMR) spectroscopy, supplemented with Diffusion Ordered Spectroscopy (DOSY) studies. Solid-state structures illustrate the conformational changes within hydrogen bonding interactions.

#### **Results and Discussion**

### Synthesis of NiL<sup>3,3'-O</sup>, NiL<sup>3,3'-S</sup>, and NiL<sup>5-O</sup>

The synthesis of the symmetric (thio)urea functionalized salen ligands and their respective nickel(II) complexes are detailed in **Scheme 1**. The synthetic route begins with 1-(3-amino-2-hydroxyphenyl)ethanone. The amine group in the 3-position undergoes facile nucleophilic addition with phenyl isocyanate or phenyl isothiocyanate to produce **HL**<sup>3-O</sup> or **HL**<sup>3-S</sup> respectively. Initial attempts to synthesize the ligand using the salicylaldehyde precursor, as opposed to the phenylethanone, were not successful due to the spontaneous self-condensation of the amine group with the aldehyde, leading to intractable products. Condensation of the acetophenone with ethylenediamine forms the ligands **H**<sub>2</sub>**L**<sup>3,3'-O</sup> and **H**<sub>2</sub>**L**<sup>3,3'-S</sup>. The ligands **H**<sub>2</sub>**L**<sup>3,3'-O</sup> and **H**<sub>2</sub>**L**<sup>3,3'-O</sup> and **H**<sub>2</sub>**L**<sup>3,3'-S</sup> were subsequently metalated with Ni(CH<sub>3</sub>COO)<sub>2</sub>•4H<sub>2</sub>O, producing **NiL**<sup>3,3'-O</sup> and **NiL**<sup>3,3'-S</sup> respectively.

Additionally, an unsymmetric ligand was synthesized to understand structural effects on the binding properties of the urea receptor (**Scheme 2**). Installation of the urea group at the 5-position was desired as a means to determine whether there

Journal Name ARTICLE

are significant changes to the anion binding behavior at a position where there would be minimal steric and electronic interactions with the nickel(II) center and the primary coordination sphere. Hydrogenation of 1-(2-hydroxy-5-nitrophenyl)ethanone afforded the aniline precursor, 5-NH<sub>2</sub>, that undergoes nucleophilic addition with phenyl isocyanate in the next step to form  $HL^{5-0}$ . Following a previously reported strategy to synthesize unsymmetric salen ligands, 2-methylpropane-1,2-diamine was used as the bridging diamine for the mono-condensation to afford  $HL^{5-0}NH_2$ . <sup>26,28</sup> Salicylaldehyde was added under reflux conditions to generate the ligand  $H_2L^{5-0}$ , and metalation was achieved with the addition of Ni(CH<sub>3</sub>COO)<sub>2</sub> •4H<sub>2</sub>O under refluxing acetonitrile.

These complexes, ligands, and their synthetic intermediates were characterized by high resolution mass spectrometry and <sup>1</sup>H and <sup>13</sup>C NMR spectroscopy. Additional characterization of the nickel complexes by single crystal X-ray diffraction is also described.

#### X-ray crystallography

Solid-state structures of the complexes NiL3,3-0, NiL3,3-5, and NiL<sup>5-O</sup> were obtained using single-crystal X-ray crystallography, providing insight into their binding properties in the presence of hydrogen bond accepting solvents. Single crystals of NiL3,3'-O suitable for X-ray crystallography were obtained from a saturated solution in deuterated dimethylsulfoxide (DMSO- $d_6$ ) and from slow evaporation of a solution of NiL3,3'-0 in tetrahydrofuran (THF). Both structures include the solvent within hydrogen bonding distance of the urea units. The DMSO $d_6$  bound structure, NiL<sup>3,3'-O</sup>•DMSO- $d_6$ , exhibits a 1:1 binding stoichiometry between the host nickel complex and the solvent guest (Fig. 1a). The DMSO- $d_6$  molecule is positioned out-ofplane from the metal complex. Hydrogen bond distances and angles are not equivalent between chemically equivalent N-H units, with N···O bond distances ranging from 2.5-3.5 Å (Table **S6**). The bond metrics indicate that the hydrogen bonds are within the moderate to strong hydrogen bonding regime, where the hydrogen bond is driven by electrostatic and covalent forces.<sup>29</sup> Similar behavior was found in the structure of NiL<sup>3,3'</sup>**s**•**DMSO** obtained from the slow vapor diffusion of methyl *tert*butyl ether into a solution of NiL<sup>3,3'-s</sup> in DMSO (Figs. 2 and S1, Table S7).

In contrast, the solid-state structure obtained from THF (NiL³,³'-O•(H²O)₂(THF)₂) shows water molecules bound to the urea in a 1:2 stoichiometry (Fig. 1b). Each water molecule also acts as a hydrogen bond donor to the oxygen atom of THF. The hydrogen bonds between water and THF are shorter and with bond angles closer to 180° compared to the hydrogen bond between water and the urea units, suggesting a more covalent hydrogen bonding nature between water and THF (Table S8). The structure obtained thus presents the possibility of stronger extraneous hydrogen bonding existing in the proximity of the nickel complex driven by the adventitious water molecules present.

Up to this point, recrystallization of the metal complexes was conducted in hydrogen bond accepting solvents. The

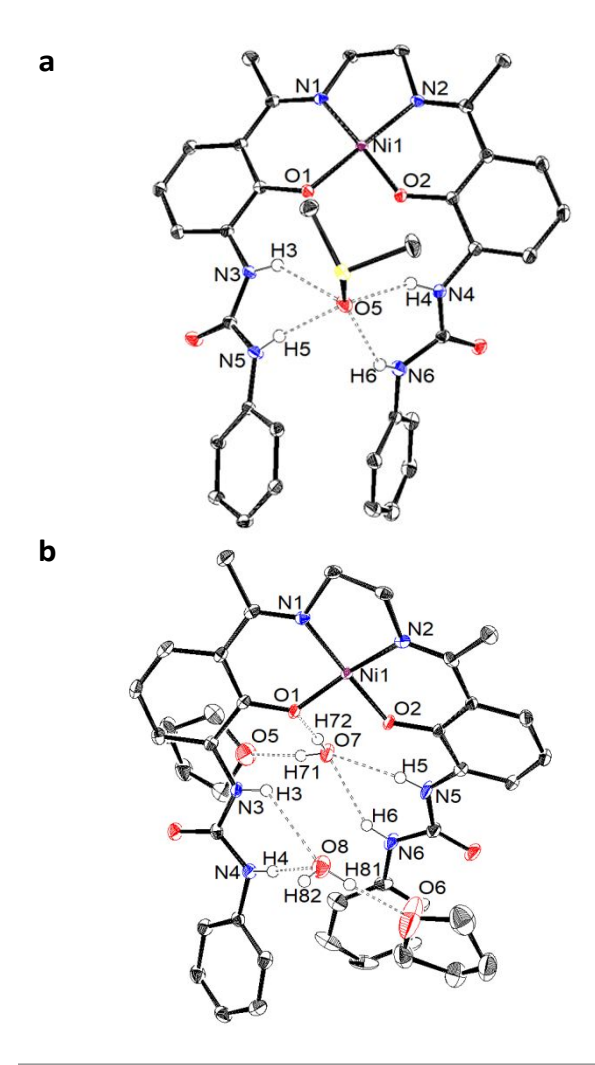
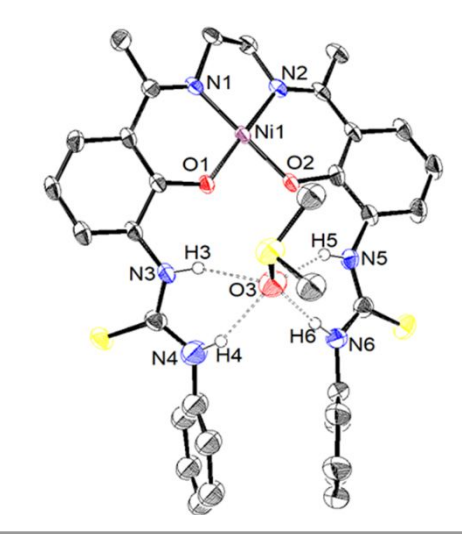


Figure 1. Solid state structures of (a) NiL³,3'.0•DMSO-d<sub>6</sub> and (b) NiL³,3'.0•(H<sub>2</sub>O)<sub>2</sub>(THF)<sub>2</sub>. Hydrogen atoms that do not participate in hydrogen bonding have been omitted for clarity. Thermal ellipsoids are represented at 50% probability.



**Figure 2.** Solid state structure of **Nil.**<sup>3,3′-5</sup>•**DMSO**. Hydrogen atoms that do not participate in hydrogen bonding have been omitted, and half of the asymmetric unit is displayed for clarity. The full asymmetric unit can be found in **Fig. S1**. Thermal ellipsoids are represented at 50% probability.

complex NiL<sup>5-O</sup> was recrystallized from the slow evaporation of its saturated solution in ethanol. The solid-state structure of

ARTICLE Journal Name

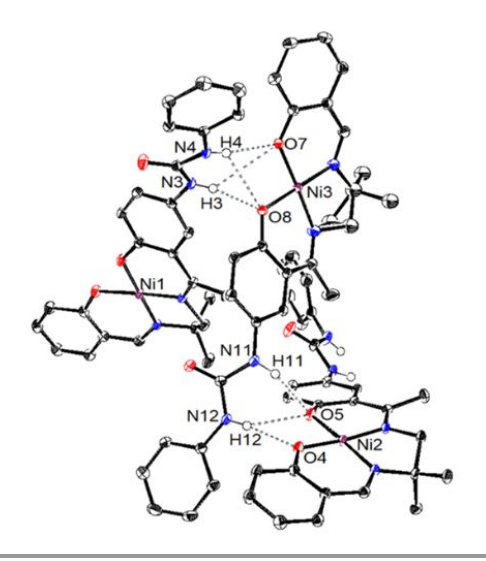


**Figure 3.** Solid state structure of **NiL**<sup>5-0</sup>. Hydrogen atoms that do not participate in hydrogen bonding and non-hydrogen bonding outer-sphere solvents have been omitted for clarity. Thermal ellipsoids are represented at 50% probability.

**NiL**<sup>5-O</sup> shows that it arranges as a trimer, whereby the urea groups are positioned within hydrogen bonding distance to the phenoxo unit of the salen scaffold (**Fig. 3** and **Table S9**). This structure demonstrates that strong intermolecular stabilization *via* hydrogen bonding can be present between the nickel(II) complexes. Furthermore, the solid-state structures obtained for

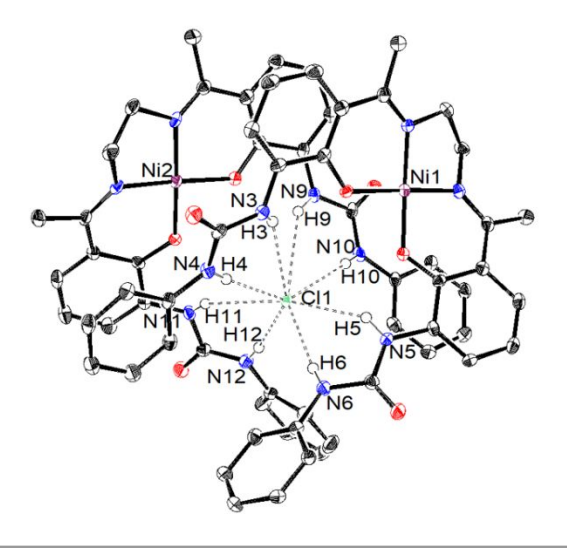


Figure 4. Solid state structure of [NiL³,3'-0]₂•Cl⁻. Outer-sphere THF molecules, the tetrabutylammonium counter-ion, and hydrogen atoms that do not participate in hydrogen bonding have been omitted for clarity. Thermal ellipsoids are represented at 50% probability.

**NiL**<sup>3,3'-0</sup> and **NiL**<sup>5-0</sup> emphasize the importance of the choice of solvent in favoring or disfavoring certain hydrogen bond pairs.

Crystallographic data was also obtained for the Cl<sup>-</sup> bound complex of  $NiL^{3,3'-O}$ ,  $[NiL^{3,3'-O}]_2 \bullet Cl^-$ , via slow evaporation in the presence of excess TBACl in THF. The Cl<sup>-</sup> atom sits between two  $NiL^{3,3'-O}$  complexes stacked perpendicular to each other in a 2:1 host:guest stoichiometry (Fig. 4). The solid-state structure of the Cl<sup>-</sup> bound complex shows the Cl<sup>-</sup> atom binding closer to the N-H units further from the nickel center ( $N_a$ -H: N4, N6, N10, N12) compared to the proximal N-H units ( $N_b$ -H: N3, N5, N9,

N11). The average bond distance of  $N_a\cdots Cl^-$  is 3.237(6) Å compared to  $N_b\cdots Cl^-$  with 3.543(3) Å (**Table S10**).

#### Anion binding studies

The nickel(II) complexes exhibit anion binding properties towards  $F^-$ ,  $Cl^-$ ,  $H_2PO_4^-$ , and  $CH_3COO^-$ . Anion binding was observed by  $^1H$  NMR spectroscopy, and all binding events were in the fast exchange regime on the NMR spectroscopic timescale except for the interaction between  $F^-$  and the symmetric complexes. The complexes were insoluble in acetonitrile, methanol, dichloromethane, and chloroform. Therefore, titration experiments were performed using DMSO- $d_6$ . Stronger binding was observed across all complexes towards  $H_2PO_4^-$  and  $CH_3COO^-$ , while the binding to  $Cl^-$  is significantly weaker, as demonstrated by the weaker deshielding effect (smaller downfield change in chemical shift) observed in the titration of  $Cl^-$  (Figs. 5a-c). Anion-specific titration curve plots can be found in Figs. S2-S4.

In general, the nickel(II) complexes bind anions quite weakly, given that excess equivalents of the anions are needed to reach equilibrium in the titration experiments. Furthermore, in the case of Cl-, the chemical shift continues to increase minimally past 20 mole equivalents. The weak binding observed may be due to the competitive binding between the anions and DMSO- $d_6$ , which hydrogen bonds to the (thio)urea units as observed in the solid-state structures. Binding constants to the anions observed in the fast exchange regime could not be accurately determined due to the ambiguity of the binding stoichiometry. However, comparisons can be drawn between the nickel(II) complexes. A key distinction between the symmetric and unsymmetric complexes is the difference in behavior of Na-H and Nb-H. A more dramatic downfield shift was observed for N<sub>a</sub>-H than N<sub>b</sub>-H in the symmetric complexes, whereas both N-H units shifted evenly in the unsymmetric complex (Figs. S2-S4). Considering the crystal structure observed for [NiL<sup>3,3'-O</sup>]<sub>2</sub>•Cl<sup>−</sup> in Fig. 4, it can be argued that steric effects play a role in the discrepancy between the change in chemical shifts observed. Due to the size of the anions, binding would have to occur out-of-plane and away from the steric congestion around the primary coordination sphere of the metal center.

Job plots of the titration of Cl<sup>-</sup> to the nickel(II) complexes suggest a mixed binding stoichiometry that is predominantly 1:2 [Ni(II)]:Cl<sup>-</sup> with minor contributions from a 1:3 association complex (Figs. S21-S23). Although a 1:2 stoichiometry is precedented by the solid-state structure of NiL3,3'- $^{\circ}$ •(H<sub>2</sub>O)<sub>2</sub>(THF)<sub>2</sub> (Fig. 1b), it does not correspond to the 2:1 structure observed in [NiL³,3'-0]<sub>2</sub>•Cl⁻ (Fig. 4). Furthermore, it is unclear how a 1:3 stoichiometry can be accommodated. While it is known that Job plots may produce inaccurate conclusions on binding stoichiometries, 30,31 attempts to resolve the stoichiometry herein using the suggested residual analysis method were not successful due to the marginal differences between the fitting of the data to various stoichiometric models.32 Our hypothesis is that, similar to NiL3,3'-O•(H<sub>2</sub>O)<sub>2</sub>(THF)<sub>2</sub>, water may be assisting in the binding of Cl<sup>-</sup>, especially given the weakness of Cl- binding to the nickel(II)

Journal Name ARTICLE

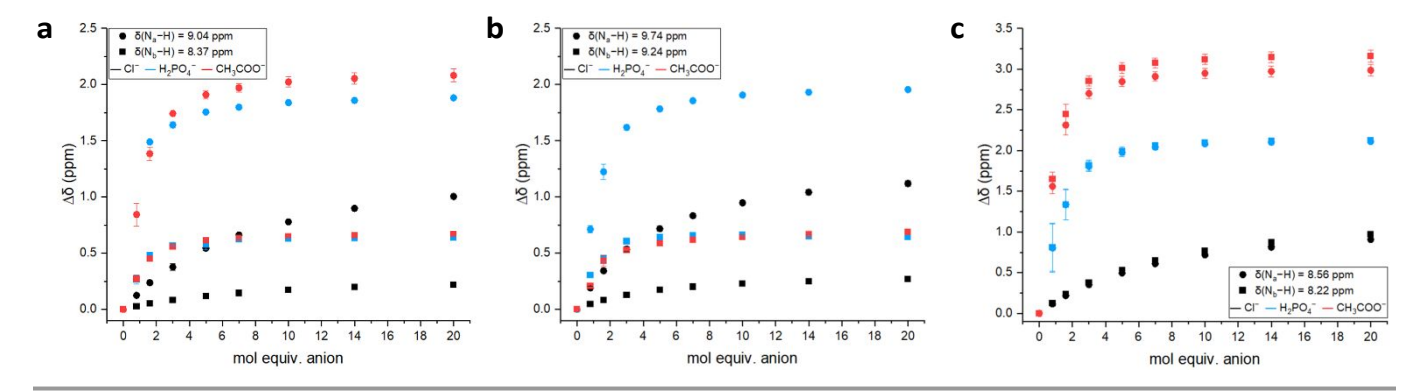


Figure 5. Titration curves for (a) NiL<sup>3,3-0</sup>, (b) NiL<sup>3,3-0</sup>, and (c) NiL<sup>5-0</sup>. The anions used are distinguished from each other by color, and the shift of N<sub>a</sub>-H and N<sub>b</sub>-H are distinguished by point shape.

complexes. The signal corresponding to water also experiences a downfield shift upon titration of Cl<sup>-</sup> (**Figs. S5-S7**). However, these changes may be a feature of dilution as a solution of TBACl in the same concentration presents the water signal at the same chemical shift (**Fig. S8**). DOSY spectra of the nickel(II) complexes in the presence of 20 mole equivalents of Cl<sup>-</sup>corroborate the participation of water in anion-bound complexes in solution (**Figs. S30-S32**). Furthermore, it is clear from the DOSY spectrum of TBACl in DMSO- $d_6$  that no interaction occurs between the deuterated solvent and the anion (**Fig. S33**). Therefore, the presence of water effectively lowers the mole fraction of the nickel(II) complex ( $\chi_{\rm H}$ ) participating in the binding interaction, making it appear as if complexes with a 1:3 binding stoichiometry exist in solution when 1:2 complexes are likely being formed.

As steric interactions appear important for the binding of Cl-, titration experiments with F- were performed to determine if a smaller anion would elicit a simpler binding behavior with the nickel(II) complexes. Indeed, NiL<sup>3,3'-O</sup> binds F<sup>-</sup> in a 1:1 stoichiometry. Titration of F-into NiL<sup>3,3'-O</sup> demonstrated binding with slow exchange kinetics relative to the NMR timescale (Fig. **S9**), as shown by the gradual disappearance of the N-H signals at 9.04 and 8.37 ppm with the concomitant appearance of doublets at 13.31 ( ${}^{1}J_{H-F}$  = 67 Hz) and 9.69 ppm ( ${}^{1}J_{H-F}$  = 19 Hz). The binding of F<sup>-</sup> can also be observed through <sup>19</sup>F NMR spectroscopy (Fig. S10), where the bound F- appears at -84 ppm as a triplet of triplets ( ${}^{1}J_{H-F}$  = 69, 22 Hz). This spectrum confirms that all four protons of the urea are binding to the anion, and there remains a spatial preference to bind closer to Na-H. A doublet at -142 ppm ( ${}^{1}J_{H-F}$  = 121 Hz) also appears in the  ${}^{19}F$  NMR spectrum, which has a corresponding triplet in the <sup>1</sup>H NMR spectrum at 16.11 ppm ( ${}^{1}J_{H-F}$  = 123 Hz) indicating the formation of HF<sub>2</sub><sup>-.33</sup> Further titration of F<sup>-</sup> results in the growth of the signals corresponding to HF<sub>2</sub><sup>-</sup> and the free F<sup>-</sup> at -101 ppm, whereas the signal of the bound F- has been extinguished to the level of noise (Fig. S11). Altogether, the data points towards a two-step equilibrium process where the binding of F- occurs first, being a prerequisite to the second equilibrium that is the deprotonation of the urea to form HF2-. The deprotonation of anion binding units by the presence of excess F<sup>-</sup> is precedented for both organic and organometallic hosts.<sup>34-41</sup> The binding constant for F<sup>-</sup> to NiL<sup>3,3-O</sup> is determined to be  $362 \pm 58 \text{ M}^{-1}$ ,

which is weak relative to binding constants that have been reported in literature among (thio)urea receptors. <sup>41</sup> However, the authors would like to note that only data points between 0.08-0.24 mole equivalents of F<sup>-</sup> was used for the calculation. Subsequent titrations led to the broadening of the N–H signals which limit the precise determination of the integration values used in the calculation of the binding constant.

The titration of F<sup>-</sup> into **NiL**<sup>3,3'-S</sup> followed a similar pattern, where the binding of F<sup>-</sup> can be observed in the slow-exchange timescale (**Fig. S12**). The  $^1$ H NMR signals corresponding to the formation of the bound F<sup>-</sup> species were found as doublets at 14.04 ( $^1$ J<sub>H-F</sub> = 71 Hz) and 10.73 ( $^1$ J<sub>H-F</sub> = 22 Hz) ppm. Deprotonation also occurred for **NiL**<sup>3,3'-S</sup> to form HF<sub>2</sub><sup>-</sup>. Unfortunately, a well-resolved  $^{19}$ F NMR spectrum could not be obtained. Therefore, it cannot be ascertained whether the binding to **NiL**<sup>3,3'-S</sup> is of a 1:1 or a 1:2 stoichiometry.

The anion binding behavior of  $NiL^{5-O}$  with F<sup>-</sup> varied from the symmetric complexes in that the exchange is fast compared to the NMR spectroscopic timescale (Fig. S13). The N–H signals decreased in intensity and broadened while simultaneously shifting downfield with the titration of the anion, indicating that the binding of the F<sup>-</sup> occurs as well as the deprotonation of the urea units. The H<sub>2</sub>O signal in the <sup>1</sup>H NMR spectrum also shifts downfield. However, H<sub>2</sub>O does not form a hydrogen bond with  $NiL^{5-O}$ , unlike that of the binding with Cl<sup>-</sup>. Instead, the DOSY spectrum indicates that the water molecules are hydrogen bonded to HF<sub>2</sub><sup>-</sup> (Fig. S34).

On the other hand, the binding of Br to the nickel(II) complexes supports the hypothesis that steric factors affect the binding affinity between the symmetric and unsymmetric complexes. <sup>1</sup>H NMR spectra of the nickel(II) complexes with 20 mole equivalents of TBABr display minimal changes in the chemical shift of the (thio)urea groups in NiL<sup>3,3'-0</sup> and NiL<sup>3,3'-5</sup>. However, a downfield shift of 0.5 ppm was observed in NiL<sup>5-0</sup>, comparable to that observed in the binding of Cl<sup>-</sup> (Fig. S14). Therefore, without the steric encumbrance presented by being near the primary coordination sphere, larger anions such as Br are better bound by the unsymmetric complex.

Titration of  $H_2PO_4^-$  to the nickel(II) complexes resulted in substantial broadening of the  $N_a$ –H and  $N_b$ –H signals in the  $^1$ H NMR spectra (**Figs. S15-S17**). Attempts to observe the speciation of the complexes upon  $H_2PO_4^-$  binding through  $^{31}P$ 

ARTICLE Journal Name

NMR spectroscopy were unsuccessful, as the fast exchange of the H<sub>2</sub>PO<sub>4</sub><sup>-</sup> ions in solution resulted in a single broad resonance in the <sup>31</sup>P NMR spectra. Broadening of the signals was even more exacerbated upon the titration of CH<sub>3</sub>COO<sup>-</sup>. The extreme case was observed in  $NiL^{3,3'-s}$ , where the signal for  $N_a-H$ disappeared immediately upon addition of CH<sub>3</sub>COO<sup>-</sup>, indicating that deprotonation occurred (Fig. S19). The signal for Na-H broadened significantly upon the addition of 0.8 mole equivalents of  $CH_3COO^-$  for both  $NiL^{3,3'-O}$  and  $NiL^{5-O}$  only to resharpen and shift downfield with further titrations of the anion (Figs. S18 and S20). Based on these observations, the  $pK_a$ of the thiourea protons of NiL<sup>3,3'-S</sup> is estimated to be below 12.3 in DMSO, while NiL3,3'-O and NiL5-O are slightly above 12.3.42,43 These  $pK_a$  values place the acidity of the nickel(II) complexes on par with the acidity of organic (thio)ureas possessing multiple trifluoromethyl substituents.44

Job plot analysis of the addition of  $H_2PO_4^-$  to the nickel(II) complexes show the maxima at approximately 0.4, indicating that the solution contains a mixture of 1 or 2  $H_2PO_4^-$  ions bound to the nickel(II) complex (**Figs. S24-S26**). Although the  $H_2O$  signal also shifts downfield and broadens upon titration of  $H_2PO_4^-$ , DOSY analysis shows that  $H_2O$  does not diffuse at the same rate as the nickel(II) complexes, implying that water is not directly bound to the (thio)urea units (**Figs. S35-S37**). The stoichiometry may be explained by a  $H_2PO_4^-$  ion binding to the nickel(II) complex as a hydrogen bond acceptor, and to a secondary  $H_2PO_4^-$  ion as a hydrogen bond donor through the protonated hydroxyl units.  $^{36,37}$  This mode of binding has been observed before in the amide-functionalized uranyl salen complexes developed by Reinhoudt and coworkers.  $^{17}$ 

Similarly, Job plots of the addition of  $CH_3COO^-$  also display a maxima at approximately 0.4 (**Figs. S27-S29**). Similar to  $H_2PO_4^-$ , the signal for water shifts downfield and broadens upon titration of  $CH_3COO^-$ , but the DOSY experiments indicate that water is not directly bound to the nickel(II) complexes (**Figs. S38-S40**). In certain cases,  $CH_3COO^-$  sufficiently basic to deprotonate the anion binding unit, forming  $CH_3COOH$ , which can subsequently hydrogen bond with  $CH_3COO^-$ .  $^{36,37,43}$  The DOSY spectrum of  $NiL^{3,3'-5}$  in the presence of 20 mole equivalents of  $CH_3COO^-$  shows disparate diffusion signals for the  $N_a-H$  and  $N_b-H$  (**Fig. S39**), which supports the hypothesis that  $CH_3COO^-$  deprotonates the anion binding unit to form an  $CH_3COOH\cdots OOCCH_3$  dimer.

#### **Conclusions**

A facile synthesis of salen ligands with symmetric (thio)urea and unsymmetric urea groups is reported using a more stable ketone precursor. The corresponding nickel(II) complexes, as well as the Cl<sup>-</sup> bound dimer of  $NiL^{3,3'-0}$ , were synthesized and structurally characterized using single-crystal X-ray crystallography. The nickel(II) complexes displayed hydrogen bonding in the solid-state, with hydrogen bond accepting solvent molecules. The most notable interaction was the binding of  $NiL^{3,3'-0}$  with two  $H_2O$  molecules, which also acted as hydrogen bond donors to the THF molecules present in the solution.

Anion binding was observed under <sup>1</sup>H NMR spectroscopy for F<sup>-</sup>, Cl<sup>-</sup>, Br<sup>-</sup>, H<sub>2</sub>PO<sub>4</sub><sup>-</sup>, and CH<sub>3</sub>COO<sup>-</sup>. The anion binding behavior of the nickel(II) complexes varied depending on the  $pK_a$  of the anion, owing to the unexpected acidity of the (thio)urea units. Binding to Cl<sup>-</sup>was weak and convoluted by the binding of water to the nickel(II) complexes. The more basic anions, H<sub>2</sub>PO<sub>4</sub><sup>-</sup> and CH<sub>3</sub>COO<sup>-</sup>, were bound stronger by the nickel(II) complexes, and the dimerization of anions upon binding occurs. The highly basic F<sup>-</sup> initially binds to the symmetric complexes, leading to deprotonation and subsequent formation of the HF<sub>2</sub><sup>-</sup> anion. The size of the anions also plays a role, with F<sup>-</sup> binding the strongest, followed by Cl<sup>-</sup> and finally Br<sup>-</sup>. Furthermore, binding to Br<sup>-</sup> is facilitated by the unsymmetric complex due to the decreased steric congestion at the 5-position. The work herein highlights the importance of  $pK_a$  and the unexpected role of solvents towards anion binding. Additionally, the ease of installation of hydrogen bond donors on the salen ligand may expand the ability of metal salen complexes to perform precise and favorable chemical transformations.

#### **Author Contributions**

J.E.L.P, N.G.L., and J.Y.Y. conceived the project. J.E.L.P. synthesized all compounds, performed all experiments, and wrote the manuscript. J.E.L.P. and J.Y.Y. analyzed the data. J.Y.Y. supervised the project and provided feedback on the manuscript. J.E.L.P., L.M.A.S., and J.W.Z analyzed the single crystal x-ray diffraction data.

#### **Conflicts of interest**

The authors declare no conflict of interest.

#### Acknowledgements

J.EL.P. would like to thank Dr. Ryan P. King for helpful discussions on synthetic strategies, Joseph Q. Nguyen for assistance with obtaining crystallographic data, and Dr. Suvrajit Sengupta for assistance with the DOSY experiments. We wish to thank the UCI Mass Spectrometry Facility for assistance with accurate mass measurements. This work was funded by award #2102589 from the National Science Foundation.

#### References

- 1 P. Chakrabarti, J. Mol. Biol., 1993, 234, 463–482.
- T. Sato, H. Konno, Y. Tanaka, T. Kataoka, K. Nagai, H. H. Wasserman and S. Ohkuma, *J. Biol. Chem.*, 1998, 273, 21455–21462.
- A. Trotta and E. N. Jacobsen, in *Anion-Binding Catalysis*, 2022, pp. 141–159.
- J. N. H. Reek, B. de Bruin, S. Pullen, T. J. Mooibroek, A. M. Kluwer and X. Caumes, *Chem. Rev.*, 2022, **122**, 12308–12360
- N. Busschaert, C. Caltagirone, W. Van Rossom and P. A.
   Gale, Chem. Rev., 2015, 115, 8038–8155.
- 6 J. Zhao, D. Yang, X.-J. Yang and B. Wu, Coord. Chem. Rev.,

Journal Name ARTICLE

- 2019, **378**, 415–444.
- 7 P. F. Lito, J. P. S. Aniceto and C. M. Silva, *Water, Air, Soil Pollut.*, 2012, **223**, 6133–6155.
- P. J. Smith, M. V. Reddington and C. S. Wilcox, *Tetrahedron Lett.*, 1992, **33**, 6085–6088.
- 9 V. Amendola, D. Esteban-Gómez, L. Fabbrizzi and M. Licchelli, *Acc. Chem. Res.*, 2006, **39**, 343–353.
- 10 A. Bianchi, K. Bowman-James and E. García-España, Eds., Supramolecular Chemistry of Anions, John Wiley & Sons, 1997.
- 11 P. D. Beer, Acc. Chem. Res., 1998, **31**, 71–80.
- 12 P. A. Gale, Chem. Commun., 2011, 47, 82–86.
- 13 R. M. Clarke and T. Storr, *Dalton Trans.*, 2014, **43**, 9380–9391.
- 14 P. G. Cozzi, Chem. Soc. Rev., 2004, **33**, 410–421.
- 15 C. M. A. Gangemi, U. Rimkaite, F. Cipria, G. Trusso Sfrazzetto and A. Pappalardo, *Front. Chem.*
- D. M. Rudkevich, W. P. R. V Stauthamer, W. Verboom, J. F. J. Engbersen, S. Harkema and D. N. Reinhoudt, *J. Am. Chem. Soc.*, 1992, **114**, 9671–9673.
- D. M. Rudkevich, W. Verboom, Z. Brzozka, M. J. Palys, W. P. R. V. Stauthamer, G. J. van Hummel, S. M. Franken, S. Harkema, J. F. J. Engbersen and D. N. Reinhoudt, *J. Am. Chem. Soc.*, 1994, **116**, 4341–4351.
- M. M. G. Antonisse, B. H. M. Snellink-Ruël, I. Yigit, J. F. J. Engbersen and D. N. Reinhoudt, J. Org. Chem., 1997, 62, 9034–9038.
- 19 M. M. G. Antonisse, B. H. M. Snellink-Ruël, A. C. Ion, J. F. J. Engbersen and D. N. Reinhoudt, *J. Chem. Soc. Perkin Trans.* 2, 1999, 1211–1218.
- 20 H. A. Miller, N. Laing, S. Parsons, A. Parkin, P. A. Tasker and D. J. White, *J. Chem. Soc. Dalt. Trans.*, 2000, 3773–3782.
- 21 R. A. Coxall, L. F. Lindoy, H. A. Miller, A. Parkin, S. Parsons, P. A. Tasker and D. J. White, *Dalton Trans.*, 2003, 55–64.
- 22 K. Nakano, T. Kamada and K. Nozaki, *Angew. Chem. Int. Ed.*, 2006, **45**, 7274–7277.
- 23 E. K. Noh, S. J. Na, S. S, S.-W. Kim and B. Y. Lee, *J. Am. Chem. Soc.*, 2007, **129**, 8082–8083.
- A. Böttcher, H. Elias, B. Eisenmann, E. Hilms, A. Huber, R. Kniep, C. Röhr, M. Zehnder, M. Neuburger and J. Springborg, *Zeitschrift für Naturforsch. B*, 1994, 49, 1089–1100.
- T. Glaser, M. Heidemeier, R. Fröhlich, P. Hildebrandt, E. Bothe and E. Bill, *Inorg. Chem.*, 2005, 44, 5467–5482.
- T. J. Dunn, C. F. Ramogida, C. Simmonds, A. Paterson, E. W.
  Y. Wong, L. Chiang, Y. Shimazaki and T. Storr, *Inorg. Chem.*,
  2011, 50, 6746–6755.
- 27 W.-D. Li, Y. Huang, S.-Z. Li and W.-K. Dong, *J. Mol. Struct.*, 2023, **1284**, 135360.
- 28 J.-P. Costes and M. I. Fernandez-Garcia, *Inorg. Chim. Acta*, 1995, **237**, 57–63.
- 29 G. A. Jeffrey, *An Introduction to Hydrogen Bonding*, Oxford University Press, 1997.
- 30 F. Ulatowski, K. Dabrowa, T. Bałakier and J. Jurczak, *J. Org. Chem.*, 2016, **81**, 1746–1756.
- D. B. Hibbert and P. Thordarson, *Chem. Commun.*, 2016,52, 12792–12805.

- 32 P. Thordarson, Chem. Soc. Rev., 2011, 40, 1305–1323.
- 33 M. J. Chmielewski and J. Jurczak, *Chem. A Eur. J.*, 2005, 11, 6080–6094.
- 34 S. Camiolo, P. A. Gale, M. B. Hursthouse and M. E. Light, Org. Biomol. Chem., 2003, 1, 741–744.
- A. M. Costero, M. José Bañuls, M. José Aurell, M. D. Ward and S. Argent, *Tetrahedron*, 2004, 60, 9471–9478.
- 36 M. Boiocchi, L. Del Boca, D. E. Gómez, L. Fabbrizzi, M. Licchelli and E. Monzani, *J. Am. Chem. Soc.*, 2004, **126**, 16507–16514.
- M. Boiocchi, L. Del Boca, D. Esteban-Gómez, L. Fabbrizzi,
   M. Licchelli and E. Monzani, *Chem. A Eur. J.*, 2005, 11,
   3097–3104.
- 38 G. Baggi, M. Boiocchi, C. Ciarrocchi and L. Fabbrizzi, *Inorg. Chem.*, 2013, 52, 5273–5283.
- D. Maity, C. Bhaumik, D. Mondal and S. Baitalik, *Inorg. Chem.*, 2013, 52, 13941–13955.
- 40 S. O. Kang, V. W. Day and K. Bowman-James, *J. Org. Chem.*, 2010, **75**, 277–283.
- 41 M. Cametti and K. Rissanen, *Chem. Commun.*, 2009, 2809–2829.
- 42 F. G. Bordwell, Acc. Chem. Res., 1988, 21, 456–463.
- 43 C. Pérez-Casas and A. K. Yatsimirsky, *J. Org. Chem.*, 2008, **73**, 2275–2284.
- 44 G. Jakab, C. Tancon, Z. Zhang, K. M. Lippert and P. R. Schreiner, *Org. Lett.*, 2012, **14**, 1724–1727.

The data supporting this article have been included as part of the Supplementary Information including experimental methods, synthetic procedures, crystallographic information, titration curves and associated NMR spectra, Job plots, DOSY plots, and other NMR spectra. Crystallographic data for NiL<sup>3,3'-</sup> $^{\circ}$ •DMSO- $d_6$ , NiL<sup>3,3'-</sup> $^{\circ}$ •(H<sub>2</sub>O)<sub>2</sub>(THF)<sub>2</sub>, NiL<sup>3,3'-</sup> $^{\circ}$ •DMSO, NiL<sup>5-</sup> $^{\circ}$ , and [NiL<sup>3,3'-</sup> $^{\circ}$ ]<sub>2</sub>•Cl<sup>-</sup>has been deposited at the CCDC under 2379616, 2379617, 2379618, 2379619, and 2379620 and can be obtained from https://www.ccdc.cam.ac.uk/.